

Coronal Seismology by Means of Kink Oscillation Overtones

J. Andries · T. Van Doorsselaere · B. Roberts · G. Verth ·
E. Verwichte · R. Erdélyi

Received: 16 February 2009 / Accepted: 28 June 2009 / Published online: 23 July 2009
© Springer Science+Business Media B.V. 2009

Abstract The detection of overtones of coronal loop kink oscillations has been an important advance in the development of coronal seismology. It has significantly increased the potential of coronal seismology and has thus initiated important theoretical and observational

J. Andries is Postdoctoral Fellow of the National Fund for Scientific Research – Flanders (Belgium) (FWO-Vlaanderen).

J. Andries (✉)
Centre for Stellar and Planetary Astrophysics, School of Mathematical Sciences, Monash University,
3800 Victoria, Australia
e-mail: jesse.andries@sci.monash.edu.au

T. Van Doorsselaere · E. Verwichte
Centre for Fusion, Space and Astrophysics, Physics Department, University of Warwick, Coventry CV4
7AL, UK

T. Van Doorsselaere
e-mail: t.van-doorsselaere@warwick.ac.uk

E. Verwichte
e-mail: Erwin.Verwichte@warwick.ac.uk

B. Roberts
School of Mathematics and Statistics, University of St Andrews, St Andrews, Fife KY16 9SS, Scotland
e-mail: bernie@mcs.st-and.ac.uk

J. Andries · G. Verth
Centrum voor Plasma Astrofysica, Katholieke Universiteit Leuven, Celestijnenlaan 200 B, 3001
Leuven, Belgium

J. Andries
e-mail: jesse.andries@wis.kuleuven.be

G. Verth
e-mail: gary.verth@wis.kuleuven.be

R. Erdélyi
Solar Physics and Space Plasma Research Centre, University of Sheffield, Hicks Building, Hounsfield
Road, Sheffield S3 7RH, UK
e-mail: robertus@sheffield.ac.uk

improvements. New detections of overtones have been made and a reduction of the error bars has been obtained. The efforts of theoreticians to extend eigenmode studies to more general coronal loop models is no longer a matter of checking the robustness of the model but now also allows for the estimation of certain equilibrium parameters. The frequencies of the detected (longitudinal) overtones are in particular sensitive to changes in the equilibrium properties along the loop, especially the density and the magnetic field expansion. Also, attempts have been made to use the limited longitudinal resolution in combination with the theoretical eigenmodes as an additional seismological tool.

Keywords Magnetohydrodynamics (MHD) · Waves · Sun-corona · Sun-magnetic fields · Sun-oscillations

1 Introduction

The suggestion that observed coronal oscillations could be used to determine the properties of localised structures in the coronal plasma such as loops or prominences is due to Roberts et al. (1984). They related observed quasi-periodic oscillations to the fundamental modes of oscillation of magnetic tubes as derived by Edwin and Roberts (1983) (see also Zaitsev and Stepanov 1975; Ryutov and Ryutova 1976; Wentzel 1979; Roberts and Webb 1978, 1979; Wilson 1979, 1980; Spruit 1982; Cally 1986). At that time observations of oscillations in the corona were not spatially resolved, so the identification of the observed modes was largely speculative. However, even at that stage the observed oscillation periods were related to the magnetic field strength by means of the period of the kink oscillation.

Decades later, kink oscillations of coronal loops were first observed very accurately by the TRACE spacecraft (Transition Region And Coronal Explorer) (Schrijver et al. 1999, 2002; Aschwanden et al. 1999; Nakariakov et al. 1999; Aschwanden et al. 2002) (or Aschwanden et al. 2003, for an observational review). By the excellent spatial resolution of the images, there seems to be no doubt about the identification as kink mode oscillations, as these are theoretically the only modes that displace the tube axis. Hence Nakariakov and Ofman (2001) used the observed frequency to determine the strength of the local coronal magnetic field, in a similar way as suggested earlier by Roberts et al. (1984).

Seismology in general refers to the process of deducing properties of a medium by analysing properties of the oscillations or the waves travelling through the medium. It can be used to deduce properties of the sources as well, but when the aim is to learn about the medium, seismology generally compares the observed dispersion with the theoretically predicted dispersion relations (as e.g. in helioseismology). Ultimately the inversion of the observed dispersion is aimed for. With only detections of single discrete oscillation events, that kind of analysis could simply not be developed when the first loop oscillations were reported. This situation changed upon the first detection of overtones of coronal loop kink oscillations by Verwichte et al. (2004). The overtones were interpreted as longitudinal overtones and the ratio between the two frequencies was found to depart from the canonical value of 2. Thus, the observed overtones showed signatures of dispersion and hence, could be used as a seismological tool.

A word of caution on the terminology to refer to the respective overtones is appropriate here, as it seems to differ between authors. If the modes are ordered according to the number of nodes in the longitudinal direction we can in general refer to them successively as the fundamental, the first overtone, second overtone, etc. Often the word harmonic is used and this is a source of confusion. Strictly speaking ‘harmonic’ should only be used when the

frequency spectrum is equidistant, i.e. the frequencies of the overtones are exact multiples of the fundamental frequency and form a harmonic series. This is not the case here, and the word harmonic is used more loosely. In a harmonic series the fundamental is called the first harmonic, the first overtone is the second harmonic etc. On the other hand, given that it is not a harmonic series anyway, harmonic is sometimes also used as synonymous to overtone, and hence the terminology ‘second harmonic’ can be ambiguous. We would therefore like to encourage the practice of referring to the fundamental when ‘harmonic’ is used as a synonym for overtone, and avoid the word harmonic as such if it is not used in the sense of a harmonic series. Therefore, the first overtone may be referred to as ‘the first harmonic of the fundamental’ or as ‘the second harmonic’, without ambiguity.

The first detections of overtones were made at a time when the inclusion of additional equilibrium parameters in the coronal loop models and their influence on the eigenmode frequencies was receiving increased interest. However, the interest was mainly in having more insight into what determines the kink frequency and in computing more accurate values for it. Dispersion due to the width of the tube had been taken into account in the initial studies by Edwin and Roberts (1983) while Van Doorsselaere et al. (2004) had begun the investigation into the influence of curvature (for more references concerning the influence of curvature see Van Doorsselaere et al. 2009, in this issue). The theoretical development of loop oscillation models is discussed in greater detail in Ruderman and Erdélyi (2009) in this issue.

The variation of the density along the loop was also just taken into account (Díaz et al. 2004; Andries et al. 2005) and it was realised immediately that this could provide a possible explanation for the observed dispersion. Using a simple model of an isothermally stratified plasma in the loop, Andries et al. (2005) and Goossens et al. (2006) related the observed period ratio to coronal density scale height. While illustrating the potential of the observed dispersion, these studies also clarified that more effort was required both from an observational and from a theoretical side. This paper is devoted to giving an overview of the recent progress obtained in understanding, observationally and theoretically, the departure of the period ratio from its canonical value.

From an observational point of view the improvements have reduced the error bars on the observed frequencies by statistically averaging the observed time signals at different positions along a loop. Recent studies also try to incorporate as much of the observational data as possible, such as the loop inclination, non-circularity and non co-planarity (Verth et al. 2008). Moreover, the detection of loop oscillations and the determination of their frequencies is expected to benefit from the development of automated edge-tracking procedures (Jess et al. 2008).

Concerning theoretical modelling, several studies have reconsidered the influence of the density structure from different perspectives: quantifying influences of loop geometry or heating functions (Dymova and Ruderman 2006; Díaz et al. 2006), obtaining analytical dispersion relations for specific density profiles (McEwan et al. 2008), specialising to the thin tube limit (Dymova and Ruderman 2006), or including the rapid density increase at the footpoints and studying the relative influence of stratification within the loop or in the environment (Donnelly et al. 2006; Díaz et al. 2007). Most importantly, the longitudinal magnetic field variation was identified as a key quantity and its effect has been quantified (Verth and Erdélyi 2008; Ruderman et al. 2008), and works against the effect caused by longitudinal density stratification. These results have also been related to observations by Verth et al. (2008).

The period ratio may in principle be studied in detail for any mode of a coronal flux tube, be it a fast kink mode or a slow longitudinal mode (McEwan et al. 2006). While harmonics

of other modes have been reported (Nakariakov et al. 2003; Melnikov et al. 2005; Srivastava et al. 2008), mainly the kink modes have been used for seismological inversion so far.

Another interesting development concerns the use of the longitudinal eigenfunctions as seismological tools (Erdélyi and Verth 2007; Safari et al. 2007; Verth et al. 2007; Andries et al. 2009). Although its application is subject to considerably more observational uncertainty, it is most certainly an avenue that must be considered.

The paper will first discuss the detection of loop oscillations and their overtones in Sect. 2. Section 3 then describes the theoretical models that have been studied in order to explain and invert the observed period ratios while Sect. 4 is then devoted to the subject of spatial seismology. Finally a summary and discussion is provided.

2 Observations of Kink Mode Longitudinal Overtones

In this section, we review the observations of multiple harmonics of transverse oscillations in coronal loops. The detection techniques are explained and their advantages and shortcomings are discussed.

So far, most transverse loop oscillations have been detected with TRACE because that spacecraft provides the high spatial and temporal resolution necessary to observe these oscillations, which have displacement amplitudes of typically a megameter (i.e. a few pixels) and periods of typically five minutes (i.e. about ten measurements per period). These time and spatial scales indicate why it is so difficult to observe multiple loop harmonics (only a handful so far!). Indeed, if you go to the first overtone of the fundamental mode, a period of 2.5 minutes is expected. For TRACE this means that it makes roughly five measurements per period. The most favourable locations to detect the different harmonic oscillations depend on the longitudinal profile of the transversal velocity amplitude. The fundamental mode has its largest velocity amplitude at the loop top. The first overtone has a velocity node at the loop top and has its largest amplitude about halfway down the loop leg. The second overtone will have two velocity nodes, one third of the total loop length up the loop leg, with an amplitude maximum near the foot points and at the loop top. The confident identification and characterisation of the overtone relies on spatial information of the oscillation amplitude as a function of distance along the loop. However, TRACE images only provide information about the projected loop displacements and projected distance along the loop. For example an accurate localisation of the loop top is difficult. Therefore, additional information such as the line-of-sight velocity amplitude provided by spectrometers (Wang et al. 2008; Van Doorsselaere et al. 2007) and/or a 3d reconstruction of the loop geometry and the oscillation polarisation using STEREO (Verwichte et al. 2009) is extremely useful.

The most common data analysis techniques to quantify the periods of oscillations start by taking a slit in the direction of the projected polarisation of the oscillation. However, most times this corresponds to the direction perpendicular to the loop because for such a configuration the oscillation is clearest. Then, the slits are stacked in time to obtain a space-time diagram known as an $x-t$ diagram. The second step is to determine the loop position as a function of time $x_n(t_n)$, with the aid of the $x-t$ diagram. This is not a trivial procedure because of interference of variations in the line-of-sight background. Interactive, semi-automated and fully automated techniques have been applied. The time series often contains a trend, which is modelled by either a polynomial fit or a large-scale running average (ideally comparable in scale to the largest oscillation period). However, it is not always easy to distinguish the trend from the oscillation.

To obtain periods from the time series, different techniques may be used: Fast Fourier Transform (FFT), periodogram, wavelets or a fitting method. Each has its own advantages

and disadvantages. Ideally, one would want to have a confident period measurement with multiple methods.

In principle, the FFT only works for equally spaced data points, which is not always the case for coronal observations with TRACE. In case of unevenly spaced time series, interpolation may be used, but that introduces additional uncertainties. This problem may be overcome by using the periodogram method instead (e.g. Scargle 1981). The spectral resolution for both FFT and periodogram is determined from the length of the time series. Because of the associated heavy damping and the limited spatial resolution, the oscillations are only seen for 3 or 4 periods at best. The short duration of the observational run results in a wide spectral peak and large errors on the periods.

An often used approach in time series analysis is the Continuous Wavelet Transform (CWT) (e.g. Torrence and Compo 1998). The transform with the Morlet mother wavelet is especially suited to detect oscillations. Its advantage is that it can describe the amplitude and spectral evolution as a function of time. Also, it naturally ignores any linear trends. However, it does share some of the same problems as for the FFT: necessity for a evenly spaced time series, and the lack of spectral resolution.

A different method is to fit the data points with multiple damped sine functions using least squares. This method also generates large errors because the oscillation is superimposed on a larger time scale trend. The functional form of such a trend is hard to guess and will significantly influence the fitting of the oscillation.

It is straightforward to detect multiple periods with FFT and CWT, because they will be visible as extra spectral peaks. However, sometimes these spectral methods do not distinguish between different periods, because of the poor spectral resolution. Detecting the multiple periods using the fitting method is more involved. There are two approaches: one fit with multiple damped sine functions and consecutive fits using a single damped sine function. With the former method a large number of oscillation parameters have to be determined (eight for two harmonics), which can make the method unstable. For the latter approach one needs to do a fitting for the most dominant harmonic first, subtract the fit, and repeat the fitting for higher harmonics. Because of multiple fittings, larger errors will be introduced in the resulting residues.

Terradas et al. (2004) apply several other data analysis techniques to known cases, and compare the results to earlier findings. They use empirical mode decomposition, principal component analysis, and Hilbert transform. These methods are all underused in coronal oscillation analysis but may prove useful in the future to detect overtone periods with higher accuracy.

There are only a few observational cases of multiple harmonics of a transverse oscillation in a coronal loop and each publication uses a different method to determine the oscillation parameters. The first two detections were obtained by Verwichte et al. (2004). In Verwichte et al. (2004), from looking at multiple slits along the loop axis, multiple periods have been determined using the CWT corresponding to the fundamental mode and its first harmonic. Also, these harmonics have been confirmed by the amplitude profile as a function of projected distance from the loop top. However, the amplitudes of the overtones are only around or even below the spatial resolution of TRACE which may cast some doubt on the significance of the overtone signal. Moreover, the overtones are only detected by CWT and are not picked up by the fitting procedure.

Van Doorsselaere et al. (2007) also used multiple slits along the loop. They measured the multiple periods of the fundamental and first overtone using consecutive fits and ob-

Table 1 An overview of observational measurements of two periods in a coronal loop. The improved errors in the measurements of Verwichte et al. (2004) have been taken from Van Doornsselaere et al. (2007)

Source	P_1 (s)	P_2 (s)	P_4 or 5 (s)	$P_1/(2P_2)$
Verwichte et al. (2004)	448 ± 16	247 ± 6	$250\text{--}346$	0.91 ± 0.04
	387 ± 8	245 ± 8		0.79 ± 0.03
De Moortel and Brady (2007) ^b	(1038–2484)	577–672	250–346	0.90 ± 0.03
Van Doornsselaere et al. (2007)	436 ± 5	243 ± 7		0.90 ± 0.03
O’Shea et al. (2007) ^a	448	224		(1) ^{a,c}
	400	164		(1.2) ^{a,c}
	476	198		(1.2) ^{a,c}
Verth et al. (2008)	242	157		(0.77) ^c

^aThe identification as a kink-mode is uncertain

^bThe mode number identification is uncertain

^cDue to unspecified error bars the value of these measurements is limited or unclear

tained amplitudes above the instrument spatial resolution. The analysis suffers, however, from a data gap after less than two periods of oscillation. This makes the mode identification less confident and limits the confidence level of the fitting method.

De Moortel and Brady (2007) characterised the first and third or fourth overtone oscillations at four slits along the loop using one fit with three damped sine functions. There are some signatures of a fundamental mode as well but they vary widely depending on the position along the loop (hence the parenthesis in Table 1). The higher overtone could not be categorised reliably as either third or fourth. Moreover, some discussion exists about the identification of the first overtone as well. In their original paper, they state that the oscillation with the highest power is the first overtone. However, the oscillation pattern may also be consistent with a vertical fundamental mode. A very small amount of power in the fundamental mode is at odds with the results of Terradas et al. (2007). The confusion with respect to the mode identification is likely to be related to the helical geometry of the loop and remains unresolved so far (see further comments at the end of Sect. 3.1). As has been pointed out by Wang et al. (2008), due to the projection effect, even for co-planar curved loops the mode identification may be doubtful if based on imaging data from certain viewing angles.

O’Shea et al. (2007) also claim to observe multiple periodicities of kink oscillations in a single loop based on data from CDS (Coronal Diagnostic Spectrometer) on board SoHO (Solar and Heliospheric Observatory). However, they observe the oscillations in the intensity, relying on an argument by Cooper et al. (2003) where the intensity oscillations are caused by a variation of the column depth during the oscillation. It is unclear whether that argument holds in this particular configuration. The mode identification is further based upon the values of the period. In the absence of concurrent imaging observations the mode identification is therefore uncertain. Furthermore, the analysis suffers from a very low spectral resolution due to the very short duration of the time sequence. As a result the period ratio cannot be determined accurately enough to show a significant difference from the canonical value of 2.

Verth et al. (2008) recently reported another detection of both the fundamental and its first harmonic. These results were based on very low cadence data. The values are obtained as averages over the measurements along different slits (private communication) and involve

automated edge tracking procedures by Jess et al. (2008). The periods are determined by CWT and from their Fig. 2, it seems that one period dominates during the beginning of the observation, whereas the other period dominates near the end. Error estimates are not given but from inspection of their Fig. 2, they are expected to be large.

As stated before, in FFT (and also with wavelets), the error in the period is mainly determined by the length of the time series. For the fitting method, it is not as simple to see. Van Doorsselaere et al. (2007) used a Monte Carlo simulation to determine the magnitude of the error in the period. Another approach would be to use the statistical error estimates of the fitting routines. The error is also influenced by the number of slits and time series used. Verwichte et al. (2004) took as an estimate of the uncertainty of the oscillation parameters the standard deviation of the measurements from all slits. This produces a relatively large error. Van Doorsselaere et al. (2007) proposed that the errors in the period measurement can be reduced by performing the analysis in multiple slits across the loop. If it is assumed that the same period is measured, the error in the period may be reduced by a factor \sqrt{N} , where N is the number of observations. The errors for the cases studied by Verwichte et al. (2004) have been recalculated this way. This error method assumes that all measurements are equal and unbiased. Considering other sources of errors (e.g. time series generation, detrending, fitting quality), it is likely that the error realistically lies between these two approaches.

Evidently, there is still a considerable amount of uncertainty associated with each of the reported detections (mode identification, significance of the observed amplitudes or the error bars). It is worth noting that TRACE was not designed to do wave studies. The observational cadence and integration times are often not constant, making wave studies more involved. Future instruments, such as SDO/AIA, may allow for more confident detection and classification of wave modes and a better determination of the wave periods.

Apart from using the observed periods of oscillation it has been suggested that the shape of the oscillation mode along the loop may be used for seismology, an idea dubbed *spatial seismology* (Erdélyi and Verth 2007). Observationally, this is not straightforward, because only a 2D projection/integrated image of the corona is available to us which makes it non-trivial to correctly identify the position on the loop of a certain pixel. Preliminary attempts have been made to do spatial seismology by Verwichte et al. (2004) and Van Doorsselaere et al. (2007). They attempted a fit with a sine function (i.e. without stratification parameters taken into account), but failed even to get a confident estimate of the loop length. These attempts could however be more successful if one would have an accurate 3D reconstruction of a loop's geometry to correct for projection effects and departure from circular shape. The recently launched STEREO should be a great help in this regard. Already some progress has been made by Aschwanden et al. (2008) using STEREO data to employ triangulation techniques in reconstructing 3D loop geometry and quantifying possible effects such as loop non-circularity and non-coplanarity. However, as has been suggested by Wang et al. (2008), additional spectral data may be necessary to provide line of sight velocities in order to obtain an accurate picture of the polarisation.

Srivastava et al. (2008) have found multiple periodicities in brightenings of post-flare coronal loops. They attributed these periods to multiple sausage mode overtones. This is an interesting avenue for seismology using multiple periods in different modes. For those different modes, however, the theory is not as advanced as for kink modes. In fact, seismology may prove to be much more difficult using sausage mode overtones, because they are strongly dispersive (see the coronal dispersion diagram in Edwin and Roberts 1983).

3 Explanations of the Overtone Period Ratios

MHD waves in a homogeneous and unbounded medium are known to be dispersionless. Hence, overtones can be expected to be found at an exact multiple of the fundamental frequency, under the condition that there is no other lengthscale whatsoever associated with the equilibrium model. This condition is however not satisfied in the case of coronal loops. There are, apart from the length of the loop, indeed several other length scales involved in any realistic loop model. The loop has a width and a curvature radius. Moreover, the loop is not invariant along the loop axis, which also can be formulated in terms of a length scale of the longitudinal variation.

As we will discuss further, the oscillation frequencies seem to be robust with respect to several of these parameters (e.g. curvature and the finite tube width), due to the fact that the loops are very thin. The most important candidates to influence the oscillation frequencies of axial overtones are the equilibrium plasma parameters that vary along the loop axis. Most significantly are the density (representing the inertia) and the magnetic field (which represents the restoring force in these oscillations). Of these two, the density structuring along the magnetic field is most easily treated as it can be dealt with in a simple model with straight magnetic field.

In much of the corona the magnetic field pressure is much stronger than the gas pressure, and we can therefore neglect the gas pressure altogether. Furthermore, it is usual to neglect gravitational forces. This aspect deserves further attention on two grounds. First of all there is the role which gravity plays in the equilibrium configuration. Because of the strength of the magnetic field in the corona, combined with a relatively low density, gravitational forces are insufficient to influence the perpendicular variation of the magnetic field. This argument (as discussed at greater length by Dymova and Ruderman 2006) can be summarised and quantified by the relevant perpendicular length scales being smaller than v_A^2/g , which is around 400 Mm using the numbers of Dymova and Ruderman (2006). However, in the direction along the magnetic field (the direction in which the Lorentz force does not operate), gravity must be taken into account. In fact in that direction also the gas pressure should be taken into account. Together they determine the longitudinal density distribution. In the end, only the longitudinal density distribution enters in the subsequent analysis. Hence, we can take the practical attitude of considering neither gas pressure nor gravity, which leaves the longitudinal density distribution to be chosen freely. Thus within such a model the transversal loop oscillations can be studied consistently without any assumptions related to the longitudinal hydrodynamic modelling of coronal loops (including their heating).

Secondly one may wonder how important the buoyancy term is in the dynamics of the oscillation. In fact, the effect is generally believed to be small, although this has so far only been assessed by McEwan and Díaz (2007) in a straight horizontal slab model. The effects were found to be of the order of gL/v_A^2 and small under coronal conditions. However, the relevance of these results for coronal loops remains to be explored.

It must also be realised that the present modelling of coronal loop kink-oscillations assumes a static background coronal loop model. This, is surely an approximation which will need to be reconsidered. It becomes more and more clear that loops are not static but involve flows and cooling. E.g. Aschwanden and Terradas (2008) have shown recently for a number of oscillating loops that they cool down on timescales of the order of a few oscillation periods. These effects will eventually need to be considered in the theoretical models.

3.1 Finite Tube Width and Curvature

Any effect that introduces dispersion of a wave also causes the period ratio between the fundamental and the overtones to depart from their canonical harmonic values. There are

two effects, namely, finite tube width and field line curvature, that act in this way, but it transpires that the period shifts they introduce are small. Consider a straight tube model in a cold plasma where the magnetic field $\mathbf{B} = B\mathbf{e}_z$ is constant. Now using a cylindrical coordinate system (r, φ, z) the density is assumed to take the constant value of ρ_i when $r < R$ and ρ_e when $r > R$. Due to the azimuthal invariance we can consider an azimuthal dependence by a factor $\exp(im\varphi)$, where m is the azimuthal wavenumber. The solutions can be constructed for general m but only the modes for $m = 1$ displace the axis and these are therefore the only ones of relevance to the observed oscillations. Likewise we consider a temporal dependence of $\exp(-i\omega t)$. In this longitudinally invariant model we also consider a longitudinal dependence of $\exp(ik_z z)$, which we will have to relax when including longitudinal variation. The longitudinal wavenumber k_z is then related to the length of the loop ($2L$) by $k_z = \pi n/(2L)$, with $n = 1, 2, \dots$ indicating the fundamental, first overtone, etc. According to Edwin and Roberts (1983), the kink mode in this model has a phase speed v_{ph} given approximately by

$$v_{ph} = v_k(1 - A(\zeta k_z R)^2 K_0(\zeta k_z R)), \quad k_z R \ll 1, \quad (1)$$

where K_0 denotes the modified Bessel function and

$$v_k = \left(\frac{2B^2}{\mu(\rho_i + \rho_e)} \right)^{1/2}, \quad A = \frac{1}{4} \left(\frac{\rho_i - \rho_e}{\rho_i + \rho_e} \right), \quad \zeta = \left(\frac{\rho_i - \rho_e}{\rho_i + \rho_e} \right)^{1/2}. \quad (2)$$

Thus, the speed v_{ph} of an individual wave varies with the longitudinal wavenumber k_z . Equation (1) allows us to determine the period P_1 of the fundamental mode and the period P_2 of its first $n = 2$ harmonic, standing in a coronal flux tube of length $2L$. The period ratio then follows as (McEwan et al. 2006)

$$\frac{P_1}{2P_2} \approx 1 - Ax^2[4K_0(2x) - K_0(x)], \quad k_z R \ll 1, \quad (3)$$

where we have written $x = \zeta\pi(R/(2L))$. So $P_1/(2P_2)$ depends upon the ratio of the loop length $2L$ to the tube radius R and the densities ρ_i and ρ_e (through the parameters A and ζ).

Now a plot of expression (3) for $P_1/(2P_2)$ as a function of x shows that it possesses a minimum, at $x = x_m$, and this gives the largest shift from unity that the kink mode period ratio exhibits due to dispersion. The minimum in x corresponds to $R/(2L) = (2/(\kappa\pi))x_m$. The value of x_m is independent of the densities ρ_i and ρ_e , being determined solely from a transcendental relation involving Bessel functions, following from a detailed consideration of (3); specifically, $x_m \approx 0.48$. The corresponding minimum value of $P_1/(2P_2)$ is then

$$\left(\frac{P_1}{2P_2} \right)_{\min} = 1 - \frac{1}{4} \left(\frac{\rho_i - \rho_e}{\rho_i + \rho_e} \right) M, \quad (4)$$

where the constant M depends only on x_m ; specifically, $M = 0.19$. Thus, the shift in $P_1/(2P_2)$ from unity depends entirely on ρ_i and ρ_e , reaching a maximum value of $\frac{1}{4}M \approx 0.0475$ in the extreme $\rho_i \gg \rho_e$. Thus dispersion in the kink mode of a *thin* coronal flux tube produces a shift in $P_1/(2P_2)$ of at most 4.75%, with a corresponding minimum period ratio of $P_1/(2P_2) = 0.9525$ (McEwan et al. 2006). This shift in period ratio, of 0.0475, is smaller than observations indicate, suggesting that dispersive effects due to the finite thickness of the tube alone cannot account for the observed period ratios.

Similarly, the effect of curvature may be considered. The analysis by Van Doorsselaere et al. (2004) showed that for thin tubes modifications to the frequencies by curvature are second order with respect to the ratio R/L , although the modifications to the eigenfunctions

are first order in R/L . Since R/L is a few percent at most for any of the loops considered, the effect of curvature can safely be neglected (for more details see the review on curvature by Van Doorsselaere et al. 2009 in this issue). It is in a very similar way that the curvature which is necessarily associated with studying expanding flux tubes can also be neglected, and the remaining influence of the tube expansion is entirely due to the longitudinal variation of the magnetic field strength (see Sect. 3.3).

An important theoretical consequence of the curvature is that the degeneracy in the polarisation is lifted. Both Van Doorsselaere et al. (2004) and Terradas et al. (2006) remark that whereas for a straight tube the eigenmodes can be polarised in any direction perpendicular to the magnetic field, the curved loop supports two distinct eigenmodes with different frequencies. One polarised in the direction of the curvature and one polarised perpendicular to the direction of the curvature. The two distinct eigenmodes are commonly termed ‘vertical’ and ‘horizontal’. However, this distinction is of limited concern to us, since the oscillation frequencies of both modes are almost identical. If a loop is excited with a polarisation which is a mixture of both eigenmodes, it takes a very long time for both modes to get out of phase. For the short duration in which a loop is observed to oscillate, it therefore effectively oscillates in the direction of the initial mixed polarisation. Thus, practically, the situation for a curved loop is identical to that of a straight tube where *a priori* no distinction is made between oscillations with different polarisations. Note that an elliptical cross section also lifts the degeneracy and may in fact be much more important (Ruderman 2003; Erdélyi and Morton 2009).

From an observational point of view Wang et al. (2008) made clear that due to the projection effect the uncertainty in the polarisation may give rise to ambiguities in the identification of the mode number. But even more fundamentally it is an open issue how the theoretical polarisation properties generalise further to helical loops. In particular, as polarisation may change along the loop, the identification of overtones may become rather confusing. This may explain the confusion associated with the observation by De Moortel and Brady (2007).

3.2 Density Stratification

Now let us generalise the above piecewise homogeneous model to a model in which the density varies longitudinally (in a continuous manner). With an azimuthal and temporal dependence $\exp(im\varphi - \iota\omega t)$, the relevant linearised MHD equations can then be brought to the following form:

$$\mathcal{L}_A \frac{1}{r} \frac{\partial r \xi_r}{\partial r} = \left(\frac{m^2}{r^2} - \frac{\mu}{B^2} \mathcal{L}_A \right) p_T, \quad (5)$$

$$\frac{\partial p_T}{\partial r} = \mathcal{L}_A \xi_r, \quad (6)$$

$$\mathcal{L}_A \xi_\varphi = \iota \frac{m}{r} p_T. \quad (7)$$

Here the Alfvén operator is defined as:

$$\mathcal{L}_A = \rho(z) \omega^2 + \frac{B^2}{\mu} \frac{\partial^2}{\partial z^2} = \rho(z) \left(\omega^2 + v_A^2(z) \frac{\partial^2}{\partial z^2} \right), \quad (8)$$

with $v_A^2(z) = B^2/(\rho\mu)$ the square of the Alfvén speed.

The equations involve the radial and azimuthal component of the Lagrangian displacement and the Eulerian perturbation of the total pressure p_T . In (5), ξ_ϕ has already been eliminated by means of (7). The first two equations form a pair of partial differential equations for the variables ξ_r and p_T .

If we consider a density distribution which does not vary with radius r within some distance R from the tube axis, and likewise outside the radius R , then in both regions the Alfvén operator can be shifted through the radial derivative in (5) and ξ_r can be eliminated in favour of p_T . The result is:

$$\frac{\partial^2 p_T}{\partial r^2} + \frac{1}{r} \frac{\partial p_T}{\partial r} - \left(\frac{m^2}{r^2} - \frac{\mu}{B^2} \mathcal{L}_A \right) p_T = 0, \quad (9)$$

which is valid in regions without radial variation only.

We can now propose separable solutions of the form $p_T(r, z) = R(r)Z(z)$ and obtain a set of a radial and a longitudinal differential equation for $R(r)$ and $Z(z)$ separately:

$$\mathcal{L}_A Z(z) = \lambda Z(z), \quad (10)$$

$$\frac{\partial^2 R(r)}{\partial r^2} + \frac{1}{r} \frac{\partial R(r)}{\partial r} - \left(\frac{m^2}{r^2} - \frac{\mu}{B^2} \lambda \right) R(r) = 0, \quad (11)$$

with λ the separation constant. In the longitudinal direction the boundary conditions require that the amplitudes of the oscillation vanish at the footpoints. The first equation together with the line tying boundary conditions is therefore an eigenvalue problem for the Alfvén operator. Given those eigenvalues (with corresponding eigenfunctions ψ), the second equation is a Bessel equation for $R(r)$. This is fundamentally equivalent to the solution method used for homogeneous unstratified tubes, except that in that case the eigenvalue problem for the Alfvén operator was solved *a priori* by a Fourier decomposition ansatz. Hence the full solution for p_T in both the external and internal medium is given by:

$$p_T^{(\text{in})}(r, z) = \sum_{k=1}^{+\infty} A^{(\text{in}, k)} I_m(\kappa_{\text{in}, k} r) \psi^{(\text{in}, k)}(z),$$

$$p_T^{(\text{ex})}(r, z) = \sum_{k=1}^{+\infty} A^{(\text{ex}, k)} K_m(\kappa_{\text{ex}, k} r) \psi^{(\text{ex}, k)}(z), \quad (12)$$

where I_m and K_m are the modified Bessel functions of the first and second kind of order m . The $A^{(\text{in, ex}, k)}$ are arbitrary coefficients of each of the Alfvén eigenmodes in the solution.

The root of $\kappa^2 = -\frac{\mu}{B^2} \lambda$ has to be taken so that it has a positive real part in order to ensure that the solution does not become unbounded at infinity. For negative values of κ^2 it is more appropriate to formulate the external solutions in terms of Hankel functions, where in fact both contributions from the Hankel function of the first and second kind have to be retained. For frequencies where this situation arises the problem is underdetermined resulting in a continuous part in the eigenmode spectrum associated with the leakage of the waves in the external medium. More frequently however only one of the Hankel functions is retained relying on the Sommerfeld outgoing radiation condition (e.g. Cally 1986). That practice leads to the determination of radiatively damped complex frequency solutions. The relation between the damped complex frequency solutions and the leaky continuous spectrum was discussed in detail by Andries and Goossens (2007) in a (longitudinally invariant) slab model. The frequencies of the fundamental and the first overtone generally do not reside in

the leaky regime although Donnelly et al. (2006) and Díaz et al. (2007) found that higher overtones are more likely to be leaky under coronal conditions.

The corresponding solutions for ξ_r are:

$$\begin{aligned}\xi_r^{(\text{in})}(r, z) &= \sum_{k=1}^{+\infty} \frac{\kappa_{\text{in},k}}{\lambda_{\text{in},k}} A^{(\text{in},k)} I'_m(\kappa_{\text{in},k} r) \psi^{(\text{in},k)}(z), \\ \xi_r^{(\text{ex})}(r, z) &= \sum_{k=1}^{+\infty} \frac{\kappa_{\text{ex},k}}{\lambda_{\text{ex},k}} A^{(\text{ex},k)} K'_m(\kappa_{\text{ex},k} r) \psi^{(\text{ex},k)}(z).\end{aligned}\quad (13)$$

The dispersion relation now follows from a matching condition of the solutions inside and outside as both the radial displacement and the total pressure perturbation need to be continuous across the boundary. For longitudinally invariant models both the internal and external eigenmodes of the Alfvén operator reduce to Fourier modes, and the matching can be performed for each Fourier mode separately. Hence, a linear system of equations arises for the amplitudes $A^{(\text{in},k)}$ and $A^{(\text{ex},k)}$ for each k separately. In the presence of longitudinal stratification this can no longer be done and instead the full expressions (12) and (13) have to be matched as functions of z . When a certain basis for the functions in z is chosen this can be expressed as a set of matching conditions for the amplitudes of each basis function. An evident choice for a set of basis functions is the Fourier basis, as in the limit of no stratification these basis functions are also the Alfvén eigenmodes, but any other basis set can be used, e.g. Díaz et al. (2002, 2004, 2006), Donnelly et al. (2006) and Díaz et al. (2007) used the approach to calculate the eigenmodes of the Alfvén operator in both media and determine the matrix governing a change of internal to external basis by considering the mutual inner products. In any case, the condition for existence of a solution is given by the determinant of the linear system of matching conditions.

Andries et al. (2005) used the Fourier sine function basis thereby representing the longitudinal Alfvén operator as a matrix operator in that basis. Then the density stratification can also be expressed in a sine series expansion as:

$$\rho(r, z) = \rho_0(r) \left[1 + \sum_{n=1}^{+\infty} \alpha_n(r) \sin\left(\frac{n\pi}{2L}(z + L)\right) \right]. \quad (14)$$

Note that the expressions presented here slightly differ from those in Andries et al. (2005) as the loop is now taken to be of length $2L$ rather than L , and the origin is at the loop apex rather than at one of its footpoints, in order to be consistent with notation used furtheron.

Within this formalism it is a tedious but straightforward computation to establish a linear expansion of the frequency in the stratification parameters α_n . A central quantity in the analysis is the matrix operator S_{nkl} which represents the n th amplitude in a sine series expansion of the product of the k th and l th sine basis function. In the absence of stratification the different eigenmodes correspond to the different basis sine functions and can be ordered by the number of nodes in the longitudinal direction. As soon as there is a longitudinal variation of the density this is no longer true and the longitudinal behaviour of the eigenmode will involve several sine function contributions. In fact, as the solution is not separable in the longitudinal and perpendicular directions, the number of nodes in the longitudinal direction may in general even depend on the radial position. However, as we will see shortly, for thin tubes the problem can be reduced to a second order differential equation for the longitudinal variation of the displacement of the tube boundary. Hence, in that case the modes may be ordered according to the nodes in the longitudinal direction. Also, if the stratification is

small one of the contributing sine functions is dominant and determines the number of nodes in the longitudinal direction at any radial position. We will therefore refer to the k th mode in that sense (while being aware that this may break down for very thick or very stratified loops). The linear approximation to the relative shift of the frequency of the k th mode is:

$$\frac{\delta\omega}{\omega} = -\frac{1}{2} \sum_n \alpha_n S_{nkk}. \quad (15)$$

As S_{nkk} is dependent on k it can clearly be seen that the longitudinal variation of the density is felt differently by the different axial overtones.

In fact the above result can be derived straightforwardly from basic principles. Dispersion relations for strings and/or surface waves are often derived using the concepts of generalised stiffness and generalised inertia (e.g. Lighthill 1978, Sect. 3.2), which is just a specific form of the Rayleigh-Ritz variational principle where the normal mode frequencies are found as stationary values of the Rayleigh quotient representing the ratio between the wave potential energy and wave inertia (e.g., Goedbloed and Poedts 2004, Sect. 6.4). The inertia are simply given by:

$$I = \rho |\xi|^2. \quad (16)$$

Upon integration over the domain the first order change induced by the modifications of the eigenfunctions vanishes (by the variational principle). Hence, at least if the density profile is separable in r and z , the relative modification of the frequency can directly be approximated as:

$$\frac{\delta\omega}{\omega} = -\frac{1}{2L} \int_z \delta\rho(z) \sin^2\left(\frac{k\pi(z+L)}{2L}\right) dz, \quad (17)$$

where $\delta\rho(z) = (\rho(r, z) - \rho_0(r))/\rho_0(r)$ is meant to represent the relative deviation of the longitudinal density profile with respect to the unstratified reference model. Through its summation over n , formula (15) is thus just the expression of this formula in the sine function basis. It is a straightforward consequence of the additional inertia as experienced by the k th mode. Through the different behaviour in the longitudinal direction, different modes experience a different amount of additional inertia introduced by the stratification. As will be discussed in a moment, when the tube is thin the problem can be reduced to a 1-D wave equation; and it was in this specific case that McEwan et al. (2008) pointed out the possibility of using a variational procedure to obtain approximations to the frequency shifts. A similar approach was used by Safari et al. (2007) also specialising to the thin tube. In fact, as has just been made clear, the original linear approximation obtained by Andries et al. (2005) can also be interpreted from a variational viewpoint and the method is not limited to the thin tube approximation. The values S_{nkk} appear in expression (15) not due to the specific choice of the basis, but naturally from the variational principle and the fact that the zeroth order solutions are pure sine functions. As soon as both a finite width and a non-separable density profile are considered, the variational approach, however, does require integration in the radial direction as well.

This approximate treatment provides an accurate insight in why and how the period ratio is expected to change by introduction of a small amount of longitudinal stratification. However, as loops stretch out into the atmosphere up to heights comparable to the expected density scale height, numerical calculations are required to solve the dispersion relation nonlinearly in the stratification parameters α_n .

Dymova and Ruderman (2005, 2006) simplified the eventual dispersion relation to solve by means of the thin flux tube assumption. The matching condition at the boundary can in that case be approximated by the condition:

$$\mathcal{L}_A^{\text{in}} \xi_r(r = R, z) = \mathcal{L}_A^{\text{ex}} \xi_r(r = R, z), \quad (18)$$

or

$$\left(\omega^2 + \frac{2B^2/\mu}{\rho_i(z) + \rho_e(z)} \frac{d^2}{dz^2} \right) \xi_r = 0. \quad (19)$$

This equation allows a much more direct interpretation in terms of a one dimensional wave equation with a variable wave speed, which is identified as the kink speed $\sqrt{\frac{2B^2}{\rho_i + \rho_e}}$. The thin tube approximation is very well satisfied for coronal loops and hence this method is very accurate. For all practical purposes concerning coronal loops both methods are effectively equivalent as we have discussed in Sect. 3.1.

If the observed deviation of the period ratio can be attributed to the longitudinal variation in density this brings about the possible inversion of the observed periods to the stratification parameters α_n . A general equilibrium model involves several stratification parameters α_n (in principle an infinite set) and therefore requires the detection of several overtones to constrain these parameters. Unfortunately, up till now, only two modes have been detected simultaneously: the fundamental and the first overtone. Hence only a one parameter model can be attempted at present.

An obvious candidate is to assume an isothermal atmosphere where the density falls off exponentially with distance from the solar surface. Assuming a semi-circular shape of the loop this can be projected onto the loop axis to yield a longitudinal variation of the density. Away from the loop axis the same longitudinal density variation is assumed. Within this model a one to one mapping results between the observationally determined ratio of the periods and the model parameter determining the relative height of the loop into the stratified atmosphere. This has first been done by Andries et al. (2005) and Goossens et al. (2006) for the two observations of overtones reported by Verwichte et al. (2004). Despite the enormous error bars (Fig. 1) the results were considered encouraging as they seemed to point in the direction of confirming an expected scale height of around 50 Mm. The two values obtained at that time were $65_{-38}^{+\infty}$ and 36_{-16}^{+63} . The first value could not exclude the possibility of higher density at the loop top (hence no upper value for the density scale height). The improved observational determination of the periods has brought down the error bars considerably. A similar analysis with the improved data by Van Doorsselaere et al. (2007) yields 68_{-21}^{+52} , 30_{-4}^{+5} and 109_{-21}^{+37} (the third value is for the new case studied by Van Doorsselaere et al. 2007). In fact at present the uncertainty due to the various specific assumptions in the model is likely to be more important than the observational uncertainty.

A number of studies have reconsidered the influence of the longitudinal density stratification to deepen our understanding of how it influences the periods and period ratios. A variety of profiles are used either solving the full dispersion relation or specialising to the thin tube approximation (19). Within the thin boundary assumption Dymova and Ruderman (2006) obtained analytic solutions for a specific profile while solving the thin tube equation numerically for other profiles. They conclude that the method is sensitive to the assumed longitudinal stratification profile. Dymova and Ruderman (2006) basically assume an isothermally stratified atmosphere but consider the loop to be not entirely semi-circular, which influences how the density stratification is projected on the loop. They find that these effects can have a significant influence. This was taken further by Morton and Erdélyi (2009) who considered

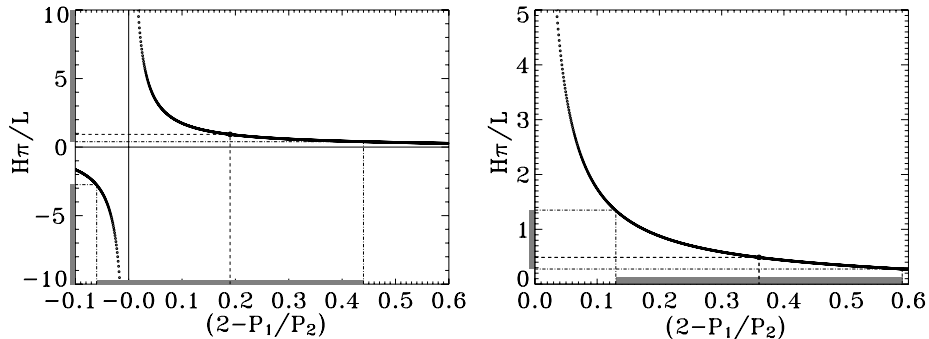


Fig. 1 The density scale height (normalised with respect to the loop height, hence $H\pi/L$) as a function of the seismological observable $2 - P_1/P_2$ for the first two cases reported by Verwichte et al. (2004). (a) The errorbars on the observed values and the estimated scale height for the first observation. As the errorbar on the measurement includes the origin, the estimate includes the possibility of a $\pm\infty$ scale height, i.e. no stratification. (b) The errorbars on the observed values and the estimated scale height for the second observation. (After Andries et al. 2005.) Here L is the full loop length and hence equivalent to $2L$ in the present notation

basically the same setup as Dymova and Ruderman (2006) but with the additional complexity that the loop may follow an elliptical trajectory rather than a semi-circular one. As in the other studies the curvature itself is not taken into account and is assumed to have negligible effect on the frequencies. Apart from a coronal density scale height, they therefore consider two additional parameters: the state of emergence (as in Dymova and Ruderman 2006) and the ellipticity. They distinguish between two cases: the ‘minor ellipse’ and the ‘major ellipse’, according to whether the vertical direction is along the minor or major axis. The deviations are found to be quite large (up to 35%) for the minor ellipse but less so for the major ellipse. The message is, clearly, that when a longitudinal density variation along the loop is related to an assumed vertical density distribution in the corona, the path of the loop through the corona has to be taken into account. Van Doorsselaere et al. (2007) show convincingly that with the improvement of the observational error bars, these effects are of comparable or even larger order than the observational uncertainties. In that respect the most recent seismological applications do take into account the various geometrical specifications of the observed loops when considering the projection of the exponential profile on the loop (Verth et al. 2008).

Both Andries et al. (2005) and Dymova and Ruderman (2006) also take into account a small intermediate layer where the density varies radially. In a longitudinally invariant loop this is known to cause damping of the oscillation by resonant absorption (Ruderman and Roberts 2002; Goossens et al. 2002). It does not, however, influence the period ratio as long as the layer is thin. More general numerical calculations were performed by Arregui et al. (2006) and Arregui et al. (2005) which show that the period ratio seems to be largely unaffected even if the radial transition layer is relatively thick. However, these computations assumed a longitudinal stratification profile independent of radial position.

Díaz et al. (2006) have considered the problem from a viewpoint of relating the frequency shifts to the heating functions. They confirmed that the dispersion due to the finite radius is negligible although they only considered the fundamental mode and did not investigate the overtone or the period ratio. A dense chromospheric footpoint layer was also taken into account by Díaz et al. (2006) (as in Díaz et al. 2004), but the analysis suffers somewhat from only taking the chromospheric layer into account in the loop interior. The effect of consid-

ering different longitudinal stratification profiles in the interior and the surrounding corona, and including a chromospheric layer both in the interior and the surrounding corona was investigated by Donnelly et al. (2006). For an exponential profile (along the loop, which is not the same as an exponential profile with height) the Alfvén eigenmode problem can be solved analytically in terms of Bessel functions of imaginary order (Díaz et al. 2007). In that study Díaz et al. (2007) also include the chromospheric layer in both interior and surrounding. Donnelly et al. (2006) and Díaz et al. (2007) point out that higher overtones may prove less useful as seismological tools as they are likely to become leaky for longitudinally stratified loops. However, no damping times were calculated. McEwan et al. (2008) have used the exponential profiles in conjunction with the thin tube approximation, upon which (19) can be solved analytically involving just Bessel functions of zeroth order.

Let us take a closer look at this analytical solution. We suppose that the plasma densities $\rho_i(z)$ inside and $\rho_e(z)$ outside the loop are exponentials with the same scale height Λ_c . We assume for simplicity that there is equilibrium symmetry about the loop apex; this allows us to consider half a loop in the region $0 \leq z \leq L$, thus $z = 0$ at the apex and $z = L$ at the footpoints. The plasma densities inside and outside the loop are then taken to be of the form

$$\rho_i(z) = \rho_i(0)e^{z/\Lambda_c}, \quad \rho_e(z) = \rho_e(0)e^{z/\Lambda_c}. \quad (20)$$

Thus, the density inside the loop is considered to increase exponentially from a value $\rho_{\text{apex}} \equiv \rho_i(0)$ at the loop apex $z = 0$ to a value $\rho_{\text{base}} \equiv \rho_i(0)e^{L/\Lambda_c}$ at the loop base $z = L$. Accordingly, the scale height Λ_c is a measure of the longitudinal structuring; it is related to the apex and base densities through

$$\Lambda_c = \frac{L}{\ln(\frac{\rho_{\text{base}}}{\rho_{\text{apex}}})}. \quad (21)$$

Thus, for example a uniform unstructured loop with $\rho_{\text{apex}} = \rho_{\text{base}}$ corresponds to $\Lambda_c \rightarrow \infty$, and a loop with $\rho_{\text{apex}} = \rho_{\text{base}}/10$ corresponds to $\Lambda_c = 0.43L$, etc.

As a consequence of this longitudinal structuring, the kink speed v_k is of the form

$$v_k(z) = v_k(0)e^{-z/(2\Lambda_c)} \quad (22)$$

and the governing differential equation for the radial displacement ξ_r becomes

$$\frac{d^2\xi_r}{dz^2} + \frac{\omega^2}{v_k^2(0)}e^{z/\Lambda_c}\xi_r = 0 \quad (23)$$

where $v_k(0)$ is the kink speed calculated at the loop apex ($z = 0$).

Equation (23) has solution (see Abramowitz and Stegun 1965, Chap. 9)

$$\xi_r(z) = A J_0\left(\frac{2\Lambda_c\omega}{v_k(0)}e^{z/(2\Lambda_c)}\right) + B Y_0\left(\frac{2\Lambda_c\omega}{v_k(0)}e^{z/(2\Lambda_c)}\right), \quad (24)$$

where J_0 and Y_0 denote the zeroth order Bessel functions.

The standing modes of oscillation of a loop of length $2L$ may be considered by applying boundary conditions to ξ_r . Line-tying at the chromospheric base requires that $\xi_r = 0$ at $z = L$. If the loops are symmetric we can exploit this symmetry and apply boundary conditions at the loop apex $z = 0$ according to the parity of the mode. For *even* modes, ξ_r is symmetric about the loop apex so $\frac{\partial \xi_r}{\partial z} = 0$ at $z = 0$; the oscillation has a maximum (or minimum) at the loop apex. Similarly, the *odd* modes have a radial displacement ξ_r that has

a node at the loop apex $z = 0$ as well as the loop base $z = L$. Notice that ‘odd’ and ‘even’ may be interpreted as referring to the longitudinal mode number. The dispersion relations that result from application of such boundary conditions involve the Bessel functions J_0 and Y_0 and their derivatives. Coronal oscillation dispersion relations of this form have been discussed by Donnelly et al. (2007) and McEwan et al. (2008).

In particular, McEwan et al. (2008) used such dispersion relations to obtain approximate expressions for the periods P_1 and P_2 of the fundamental and its first harmonic of the loop (of length $2L$) as a whole, valid for weak longitudinal structuring (i.e., the first departure from uniformity). Specifically, they showed that P_1 is determined by

$$\frac{P_{\text{kink}}}{P_1} = 1 - \left(\frac{\pi}{4} - \frac{1}{\pi} \right) \left(\frac{L}{\pi \Lambda_c} \right) + \left(\frac{\pi^2}{48} - \frac{1}{8} - \frac{1}{\pi^2} \right) \left(\frac{L}{\pi \Lambda_c} \right)^2, \quad L \ll \pi \Lambda_c, \quad (25)$$

and P_2 by

$$\frac{P_{\text{kink}}}{P_2} = 2 - \frac{\pi}{2} \left(\frac{L}{\pi \Lambda_c} \right) + \left(\frac{\pi^2}{24} - \frac{1}{16} \right) \left(\frac{L}{\pi \Lambda_c} \right)^2, \quad L \ll \pi \Lambda_c. \quad (26)$$

Here P_{kink} denotes the fundamental period of a fast kink wave in a *uniform* loop:

$$P_{\text{kink}} = \frac{4L}{c_k(0)}. \quad (27)$$

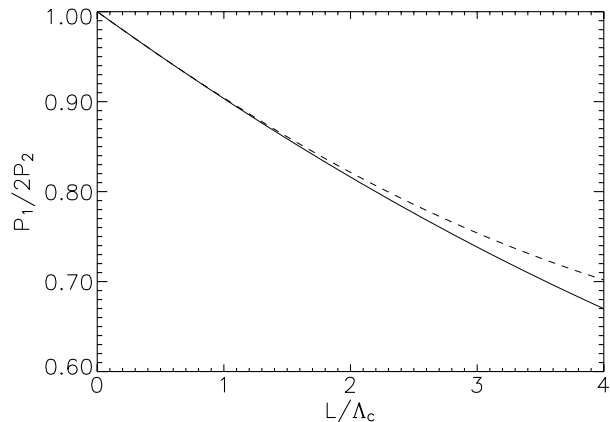
The uniform loop corresponds to the limit $\Lambda_c \rightarrow \infty$, for which (25) and (26) give $P_1 = 2P_2 = P_{\text{kink}}$. As discussed earlier at least the linear part of these results may be interpreted by the variational approach. It is easy to check that the linear part of the above expressions can be recovered by integrating (with proper normalisation) the density profile multiplied with the square of the fundamental or first overtone sine function. The second order part cannot be recovered in that way straightforwardly as this also involves the first order changes to the eigenfunctions. Expressions (25) and (26) determine, for an exponentially structured loop with density profiles given by (20), the fundamental period P_1 and the period P_2 of its first harmonic, expressed in terms of the loop length $2L$ and the kink mode period P_{kink} for a uniform loop. By forming the period ratio we may eliminate P_{kink} :

$$\frac{P_1}{2P_2} = 1 - \frac{1}{\pi^2} \frac{L}{\Lambda_c} + \left(\frac{2}{\pi^4} - \frac{5}{32\pi^2} \right) \left(\frac{L}{\Lambda_c} \right)^2, \quad L \ll \pi \Lambda_c. \quad (28)$$

Formula (28) relates the period ratio to the ratio $L/(\pi \Lambda_c)$, and so may be used to deduce Λ_c from a knowledge of the period ratio and loop length $2L$ (given the assumed model of the density profile). Figure 2 shows the variation of $P_1/(2P_2)$ with L/Λ_c as determined by (28). Also shown are the results obtained from a numerical solution of the full dispersion relations. The agreement is excellent. In fact, the approximate period ratio given by (28) agrees with the full numerical results rather better than one would have expected, given the constraint imposed by the condition $L \ll \pi \Lambda_c$. This condition is evidently satisfied for a loop with say $\rho_{\text{apex}} = \rho_{\text{base}}/2$, which corresponds to $L/\Lambda_c = 0.69$, and similarly for a loop with $\rho_{\text{apex}} = \rho_{\text{base}}/10$, giving $L/\Lambda_c = 2.30$; both these cases satisfy reasonably well the requirement that $L/(\pi \Lambda_c) \ll 1$. But for $\rho_{\text{apex}} = \rho_{\text{base}}/100$, which gives $L/\Lambda_c = 4.60$, the condition is not satisfied. Nonetheless, the trend given by formula (28) is likely to be a good guide as to more exact numerical results for arbitrary density ratios.

Not only the exponential density profile discussed above can be solved analytically. Other profiles (such as a linear one) may be treated in much the same way and in fact produce

Fig. 2 The period ratio $P_1/(2P_2)$ for a thin tube with exponential longitudinal structuring. The solid curve corresponds to the analytical approximation (28). Also shown, by a dashed curve, is the period ratio as determined by numerical solution of the dispersion relations. There is excellent agreement between numerical and analytical results. (After McEwan et al. 2008)



a similar formula for the period ratio. However, more general profiles require a numerical approach. The variational approach is illustrated as a numerical tool in McEwan et al. (2008), where it is shown that ω^2 may be expressed in terms of integrals of the eigenfunction ξ and its derivative. By choosing simple trial functions for the eigenfunction ξ , that satisfy the appropriate boundary conditions on a mode but not the differential equation itself, we may construct approximate values of ω^2 for any profile. This is an easy to implement scheme, leading essentially to the evaluation of simple integrals involving the specific density profile, and may be used to determine period ratios. It may be noticed that the scheme followed by Andries et al. (2005) is in origin not very different. In that case the trial functions are the longitudinal Fourier modes and the integrals are the Fourier transforms of the equilibrium profile. The additional complication in that scheme arises from taking into account the finite width of the tube as well. While such fully numerical calculations are clearly available, they lack the insight afforded by studying specific profiles and obtaining approximate formulae such as (28) or (15).

3.3 Tube Expansion and Variation of the Magnetic Field

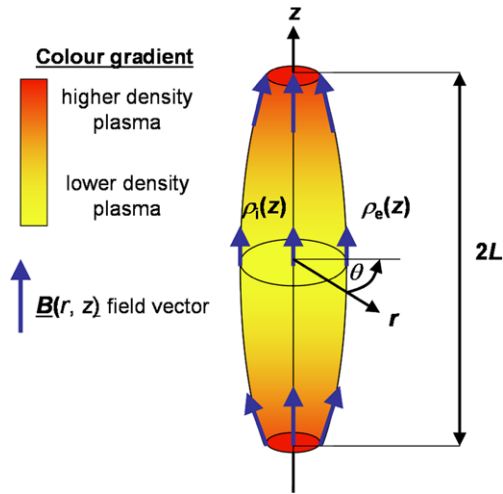
As was clear from the very beginning, also a longitudinal variation of the restoring force, i.e. the magnetic field strength, results in dispersion. However, by the solenoidal constraint longitudinal field variation necessarily involves divergence of the magnetic field lines and therefore cannot be treated in a straight geometry. Hence, geometrical effects will complicate the analysis, although the conclusion from the two studies tackling this problem seems to indicate that to lowest order, these geometrical effects are in fact unimportant as long as the tube is thin. Verth and Erdélyi (2008) and Ruderman et al. (2008) modelled an expanding potential magnetic flux tube of length $2L$ with arbitrary internal and external longitudinal densities $\rho_i(z)$ and $\rho_e(z)$ (see Fig. 3). In these models the flux tube is constructed with rotational symmetry about the z -axis and in the absence of magnetic twist:

$$\mathbf{B} = B_r(r, z)\mathbf{e}_r + B_z(r, z)\mathbf{e}_z \quad (29)$$

so that the solenoidal condition is satisfied. As before, gravity is neglected and the plasma is considered to be cold to approximate coronal conditions. The magnetic field can now conveniently be expressed in terms of a vector potential \mathbf{A} with only an azimuthal component,

$$\mathbf{A} = \frac{\psi(r, z)}{r}\mathbf{e}_\varphi. \quad (30)$$

Fig. 3 Stratification of plasma density with an inhomogeneous magnetic field. (After Verth and Erdélyi 2008)



The vector potential described by (30) is convenient since ψ is a flux function i.e. it is constant along field lines. Verth and Erdélyi (2008) showed by assuming a thin flux tube with small expansion that the equilibrium quantity B_z , in the vicinity of the tube can be given as a function of z only, to excellent approximation. In the same spatial vicinity, the relationship between the equilibrium quantities can then be approximated by the following equations,

$$\psi = \frac{1}{2}r^2 B_z, \quad (31)$$

and

$$B_r = -\frac{r}{2} B_z', \quad (32)$$

where $' \equiv d/dz$. Small tube expansion also gives the valid approximation,

$$B = \sqrt{B_r^2 + B_z^2} \approx B_z. \quad (33)$$

These approximations are used both in the analysis by Verth and Erdélyi (2008) and Ruderman et al. (2008). Whereas Verth and Erdélyi (2008) consequently follow a brute force calculation in cylindrical coordinates, Ruderman et al. (2008) somewhat more elegantly carry out the calculations in terms of the flux coordinate ψ and the azimuthal, longitudinal and perpendicular components of the displacement. In those coordinates the matching conditions at the tube boundary are more easily performed than in the cylindrical coordinate system used by Verth and Erdélyi (2008). Consequently, Ruderman et al. (2008) arrive at a dispersion relation which is of the simple Sturm-Liouville type,

$$\frac{d^2\eta}{dz^2} + \left[\frac{\omega}{v_k(z)} \right]^2 \eta = 0, \quad \eta = 0 \quad \text{at } z = \pm L, \quad (34)$$

where $\eta = \xi_\perp/r_0$ and $v_k(z) = B_z(z)/\sqrt{[\mu(\rho_i(z) + \rho_e(z))]/2}$. It is straightforwardly recognised as a generalisation of (19) which was derived for a constant magnetic field. Verth and Erdélyi (2008) arrived at a slightly different equation, although it was shown by Ruderman

et al. (2008) that the solutions to both are almost equivalent. It thus seems that the difference is of higher order in the thin tube parameter R/L .

More loosely speaking (34) suggests that to lowest approximation a thin tube behaves exactly as a string with a variable tension and density, and all geometrical effects of the tube expansion are higher order and can be neglected.

On average, the magnetic field strength is expected to decrease with height above the photosphere and the results of Lin et al. (2004) seem to confirm this. The flux tube interpretation of coronal loops suggests that most loops should expand with height above the photosphere, since flux tube cross-sectional area and magnetic field strength are inversely proportional. This expansion, defined by $\Gamma = r_a/r_f$ where r_a is the radius at the apex and r_f is the radius at the footpoint, has been estimated for a number of loops. Analysing Yohkoh data, Klimchuk (2000) measured a median value of $\Gamma \approx 1.30$ for soft X-ray loops. Using TRACE data, Watko and Klimchuk (2000) measured mean values of 1.16 and 1.20 for nonflare and post-flare EUV loops, respectively. So far, potential and force-free magnetic field extrapolations tend to predict larger loop expansions than those observed (see e.g., McClymont and Mikić 1994; Gary 1997; Klimchuk 2000; López Fuentes et al. 2006). A twisted magnetic field could reduce the amount of loop expansion with height but a force-free extrapolation of a twisted loop embedded in a magnetic dipole by Klimchuk et al. (2000) showed that although the twist did reduce the expansion of the loop, the observed relatively constant thickness could still not be matched. Alternatively it could be that the resolution of previous/current images has simply not been sufficient to observe coronal loop expansion accurately enough (see e.g., DeForest 2007). However, López Fuentes et al. (2008) strongly disagree with the idea of unresolved loop expansion and suggest that the observed near constancy of loop width is due to the magnetic field within loops being highly tangled.

Solving (34), Verth and Erdélyi (2008) found that for an expanding loop with a potential magnetic field (with free parameter, loop expansion factor $\Gamma = r_a/r_f$) and constant density, the period ratio of the fundamental mode to the first overtone can be approximated to first order by

$$\frac{P_1}{2P_2} = \left[1 + \frac{3(\Gamma^2 - 1)}{2\pi^2} \right]. \quad (35)$$

Equation (35) shows that change in period ratio is purely dependent on Γ and that $P_1/(2P_2) \geq 1$. Therefore, if magnetic field strength is decreasing with height above the photosphere, this has the *opposite effect* to that of density stratification on the period ratio (see left of Fig. 4).

Although they should be used with care due to the uncertain errorbars, two results of O’Shea et al. (2007) have $P_1/(2P_2) > 1$ which may be interpreted as kink oscillations which have the effect of loop expansion dominating over the effect of density stratification. Regarding the observational results De Moortel and Brady (2007), if we use the interpretation of De Moortel & Brady of the first overtone having the most power, then the mean value from Table 1 of their paper has $P_1/(2P_2) = 1.38$. If we assume that most of the power must be in the fundamental mode and therefore interpret P_2 and P_4 or 5 in table 1 as P_1 and P_2 , then the mean value is $P_1/(2P_2) = 1.07$. Either way both interpretations have $P_1/(2P_2) > 1$. So this may be further evidence of the effect of loop expansion dominating over density stratification. If we assume that the observed loops of O’Shea et al. (2007) and De Moortel and Brady (2007) have a constant magnetic field, then the values of $P_1/(2P_2)$ could be interpreted as loops having a negative scale height, i.e., being more dense at their apex. However, the effect of an expanding flux tube offers a physically more reasonable and simpler explanation.

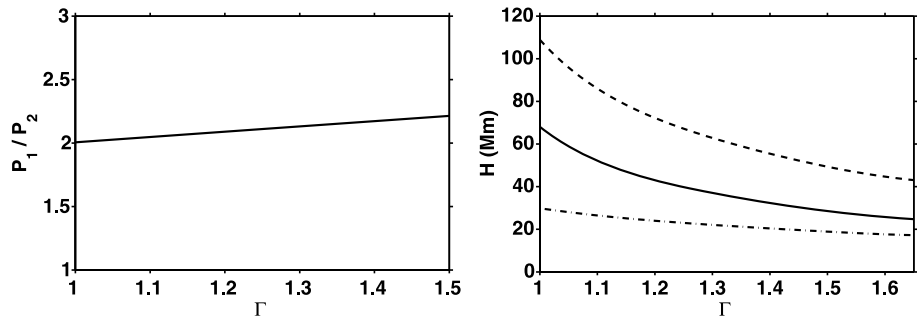
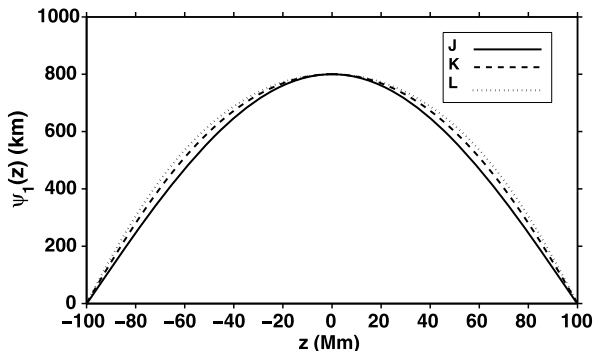


Fig. 4 *Left:* The period ratio P_1/P_2 plotted against expansion factor Γ with a constant plasma density. *Right:* The solid and dashed-dotted curves show the dependencies of the scale height H on the expansion factor Γ for the two cases reported by Verwichte et al. (2004). The dashed curve shows the dependence of H on Γ for the case reported by Van Doorsselaere et al. (2007). (After Ruderman et al. 2008)

Implementing the previously described expanding flux tube theory, we revisit three results by Andries et al. (2005) and Van Doorsselaere et al. (2007), where they used measurements of $P_1/(2P_2) < 1$ to estimate the coronal density scale height, assuming a constant magnetic field. Now we can quantify the possible corrections to these estimates due to possible loop expansion. Solving the governing equation (34) with same exponential density profile of Andries et al. (2005) and Van Doorsselaere et al. (2007), H is plotted against Γ (varying Γ from 1 to 1.65) for the three cases and the results are presented in the right panel of Fig. 4. Significantly, we see that the scale height is a decreasing function of Γ , i.e., neglecting loop expansion causes H to be overestimated. Therefore, the scale height estimates of Andries et al. (2005) and Van Doorsselaere et al. (2007) can only be taken as upper bounds.

The magnetoseismological estimates by Andries et al. (2005) and Van Doorsselaere et al. (2007) were made using TRACE 171 Å passband which has its peak response temperature around $T \approx 1$ MK. Coronal loops observed at this wavelength, if in hydrostatic equilibrium, should have $H \approx 50$ Mm. If we assume a constant magnetic field, then the two diagnosed scale heights of $H = 68$ Mm and $H = 109$ Mm represent super-hydrostatic scale heights (with the case of $H = 30$ Mm representing a sub-hydrostatic scale height). Thus far, there has been no satisfactory theoretical explanation for possible super-hydrostatic scale heights in the corona (see e.g., DeForest 2007, for detailed discussion). However, it can be seen from Fig. 4, that expansions of only $\Gamma \approx 1.1$ and $\Gamma \approx 1.5$ would result in hydrostatic scale heights for these loops. Furthermore, these values are consistent with the modest values of Γ measured by Watko and Klimchuk (2000) for TRACE EUV loops (see Figs. 14 and 15 in their paper). Unfortunately, none of the time series data of these observational examples allows for an actual visual determination of Γ since they are all only visible at small apex sections. However, there has been a recent study by Verth et al. (2008) of the TRACE Bastille Day 1998 post-flare loop oscillation data where both the ratio $P_1/(2P_2)$ and the loop expansion Γ could be estimated. The active region AR 8270, where this event took place, was predominantly bipolar in nature and the analysed loop was found to be approximately semi-circular with $\Gamma = 2.05$, consistent with a similar shaped loop embedded in an ideal dipole. Emphasising the magnetoseismological importance of correcting for loop expansion, it was found that the density scale height was reduced substantially (by a factor of 2).

Fig. 5 Longitudinal variation of the displacement amplitude for three different profiles of the longitudinal density distribution. J corresponds to a longitudinally invariant loop. For details on K and L see Erdélyi and Verth (2007). The apex maximum amplitude for the fundamental kink mode (at $z = 0$) is normalised to 800 km. (After Erdélyi and Verth 2007)



4 Spatial Seismology

Inspired by the seismological results based on the period ratio, Erdélyi and Verth (2007) suggested that it may be beneficial to attempt seismology in the spatial domain, i.e., by analysing the eigenfunctions. In theory, one could produce numerous density profiles that would result in the same period ratio $P_1/(2P_2)$. However, if one could determine the eigenfunction with enough accuracy, the seismological inversion would provide a much more unambiguous determination of the true density profile.

Implementing the valid thin flux tube approximation of Dymova and Ruderman (2006), Erdélyi and Verth (2007) made a detailed study into variation of the eigenfunction of the commonly observed fundamental mode with a realistic exponential density profile for a vertical semi-circular loop. Figure 5 shows the longitudinal variation of the displacement amplitude for varying values of the stratification parameter. The maximum eigenfunction amplitude is fixed to a typical observed value of 800 km. It can be seen from Fig. 5 that the eigenmodes of stratified loops only deviate very slightly from those of constant density. Although previously mentioned by Andries et al. (2005) this was only quantified rigorously by Erdélyi and Verth (2007). For a loop with loop half length $L = 100$ Mm and density scale height $H = 50$ Mm, the maximum change would only be about 50 km, below even the best future planned EUV resolution of SO (150 km at perihelion). These eigenfunction results were subsequently confirmed by Safari et al. (2007) using a perturbation method. They also provide computations for the modifications to the eigenmodes of the first overtone, and in fact for any overtone in general. They focus on the maximum amplitude of the modifications, which is found to be small.

Verth et al. (2007) point out that a much more promising spatial signature of density stratification is the anti-node shift of the first overtone towards the loop footpoint (as shown in Fig. 6 right). The normalised anti-node shift is linear to good approximation for expected coronal values (cf., Fig. 6 left) and for a vertical semi-circular loop is given by the simple formula

$$\frac{|\Delta z_{\text{AN}}|}{L} = 0.028 \frac{L}{H}. \quad (36)$$

Although the right hand side of (36) is relatively small, the shift may be substantial due to the large length scale of the oscillations. E.g., $L = 100$ Mm and $H = 50$ Mm causes a shift of 5.6 Mm, well within the resolution of TRACE (714 km).

This was taken up further by Andries et al. (2009) anticipating possible detection of higher overtones in the future. Carrying out a linear expansion of the eigenfunctions in the stratification parameter α (as Andries et al. 2005 had done earlier for the frequency), an

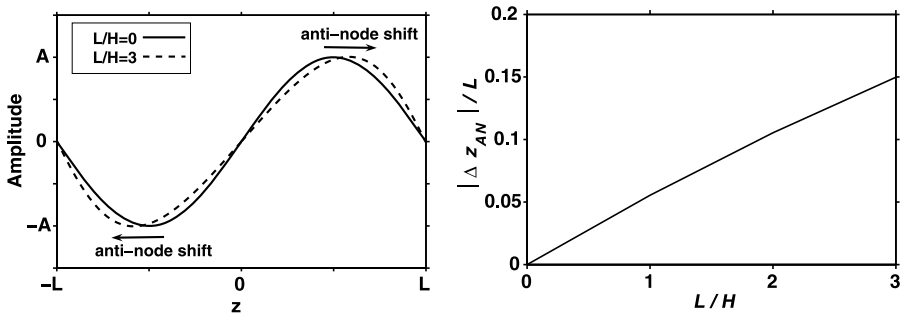


Fig. 6 *Left:* Plot showing the shift of the anti-node of the first overtone towards the loop footpoints if there is density stratification and a constant magnetic field. *Right:* Normalised anti-node shift, $\Delta|z_{AN}|/L$ against L/H for a loop with density stratification and a constant magnetic field

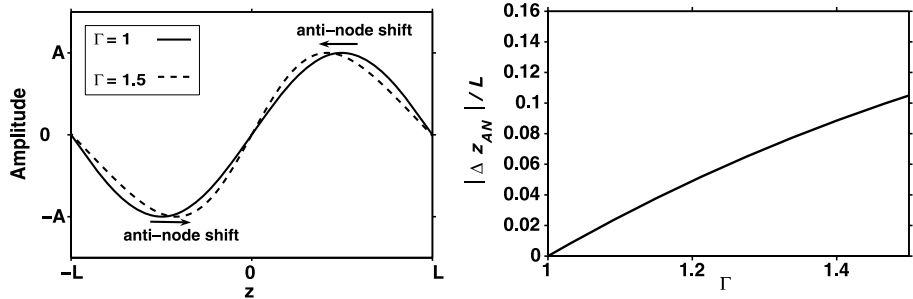


Fig. 7 *Left:* Plot showing the shift of the anti-node of the first overtone towards the loop apex if there is magnetic stratification and constant density. *Right:* Normalised anti-node shift, $\Delta|z_{AN}|/L$ against Γ for a loop with magnetic stratification and constant density

approximation is found for the l th Fourier contribution in the k th mode with k and l arbitrary. The obtained formulae are similar to those of Safari et al. (2007) but obtained in a different way and valid for both displacement and compression, which have a different longitudinal profile. The formulae are straightforwardly related to the anti-node shifts and confirm the results obtained by Verth et al. (2007). Interestingly it is found that the eigenmodes of higher overtones will be altered even more. However, they conclude that the shift of the antinode does not seem to be the best signature of the eigenfunction modifications. Moreover, the linear behaviour for relatively large values of stratification found by Verth et al. (2007) was shown to be rather specific for the density profile considered. Furthermore, they clarify that the modifications to the eigenfunction of the fundamental and the first overtone are much larger in the compression than in the displacement. Although it is unlikely that the compression can be detected very accurately, if it could be detected it would have a much larger potential.

Regarding the spatial seismological signature of loop expansion, it was shown by Verth and Erdélyi (2008) that in contrast to the effect of density stratification, magnetic stratification causes the anti-node of the first overtone to shift towards the loop apex (see right of Fig 7). The linear approximation of normalised anti-node shift for a loop with constant

density is given as a function of Γ by

$$\frac{|\Delta z_{\text{AN}}|}{L} = 0.294(\Gamma - 1). \quad (37)$$

Hence for a loop with $L = 100$ Mm, it only takes a relatively small expansion of $\Gamma = 1.2$, to create a shift of 5.9 Mm, approximately the same size of shift (but in the opposite direction) caused by a density scale height of $H = 50$ Mm. The importance of correcting for possible loop expansion when making coronal density scale height estimates from the observed value of $P_1/(2P_2)$ was previously stated in Sect. 3.3. Likewise, in the spatial domain, loop expansion must also be corrected for, along with other important factors such as loop shape and inclination.

It must be noted, that a prerequisite to *spatial seismology* is an accurate determination of the polarisation. As long as only projected amplitudes are measured, the true amplitudes remain inaccessible. This is, however, a very complicated task, and requires accurate reconstruction of the loop geometry as well as additional line of sight velocity/displacement diagnostics.

5 Conclusions and Discussion

The observation of overtones of coronal loop oscillations can clearly be considered a landmark in the area of coronal loop seismology. The first observations gave an immediate boost to the development of the theoretical models of coronal loop kink oscillations. Of the first extended models available, the longitudinal variation of the density seemed to have the most important impact on the periods of the overtones (the ratio with the fundamental period). The deviation of the period ratio from its canonical value of 2 was thus used as a seismological tool to better understand the variation of the density along the loop. The original analysis suffered from large observational uncertainties but its potential was recognised immediately. From the observational side attention was paid to the reduction of the error bars, with great success, resulting from combining time series analysis at several points along the loop.

From a theoretical side it was recognised that apart from the longitudinal density variation many other parameters could influence the period ratio, and the community embarked at an effort to assess which are the most important. It would seem that the most important effects are due to the longitudinal changes of the equilibrium parameters, most notably the density (the inertia) and the magnetic field (the restoring force).

While the variation of the magnetic field necessarily involves the consideration of flux tube expansion and hence introduces more computational complexity through the curvature of the magnetic field lines, its effect is almost entirely due to the longitudinal variation of the magnetic field strength. All direct geometrical effects on the loop oscillations are expected to be negligible as long as the loop is thin. For example, the inevitable curvature associated with the expansion is found to be negligible because the loops are thin, in agreement with the results for a curved but non-expanding flux tube.

For some observed loops the expansion of the loop can be measured with some degree of accuracy which provides a direct handle on the effect of the varying magnetic field and leaves the longitudinal variation of the density as the only remaining parameter. As a model for the density there is basically no constraint and any longitudinal profile can be proposed, relying on the specification of a heating function. As at present, with the observation of a single overtone, there seems to be no possibility in discriminating between different heating

functions, the most popular model is that of an isothermally stratified plasma. In most recent studies the effects of the loop geometry (non-circularity, non-coplanarity, inclination angle, etc.) are taken into account in that respect. For that aim it is thus worth to assemble as much information as possible about the geometries of the oscillating loops prior to attempting any seismological inversion. The 3-D reconstruction of coronal loop geometries by means of STEREO data and/or magnetic field extrapolation is thus of direct relevance to coronal loop seismology.

As the longitudinal variation of the equilibrium quantities not only modifies the eigenfrequencies but also the eigenfunctions, one could attempt to determine the longitudinal eigenfunctions profile theoretically and observationally to provide an additional seismological constraint. Attempts of this sort have so far been unsuccessful. While changes are marginal for the fundamental mode, they could be detectable for the overtones. In any case, such type of analysis has to take into account the polarisation of the oscillation, which is often hard to determine very accurately.

Neither the damping nor the excitation of the loop oscillations has been addressed specifically in this review although they remain important subjects of study as well. The excitation problem is of relevance to the present subject as the relative amplitudes of the overtones depend on the initiation parameters. Terradas et al. (2007) have investigated this theoretically and concluded that an asymmetric initiation closer to the loop footpoints favours the excitation of overtones. Nevertheless, the fundamental mode always seems to dominate. This problem has also been addressed numerically (Selwa et al. 2006) with similar results.

Somewhat contrary to helioseismology where one tries to deduce information about the variation of equilibrium quantities with depth, seismology of coronal loops by means of kink oscillation overtones is, as it stands, aimed solely at resolving longitudinal variation of the equilibrium quantities. The variation of the quantities with radius is effectively removed by the fact that the loops are thin. Observations in the corona suffer from a line of sight integration effect which makes it hard to obtain longitudinal profiles of equilibrium quantities by direct observation. The methods developed in coronal loop seismology and described in this review are therefore valuable tools in the determination of these quantities.

Acknowledgements This review was born out of the discussions that took place at the International Team Programme “Waves in the Solar Corona” of the International Space Science Institute 2009 (ISSI), Bern. The authors thank ISSI for the financial support and great hospitality received during their stay in Bern.

JA and TVD are supported by, respectively, an International Outgoing and an Intra-European, Marie Curie Fellowship within the 7th European Community Framework Programme.

RE acknowledges M. Kéray for patient encouragement and is also grateful to NSF, Hungary (OTKA, Ref. No. K67746) and the Science and Technology Facilities Council (STFC), UK for the financial support received.

References

- A. Abramowitz, I.A. Stegun, *Handbook of Mathematical Functions* (Dover, New York, 1965)
- J. Andries, M. Goossens, Phys. Plasmas **14**, 052101 (2007). doi:[10.1063/1.2714513](https://doi.org/10.1063/1.2714513)
- J. Andries, I. Arregui, M. Goossens, Astrophys. J. **624**, L57–L60 (2005). doi:[10.1086/430347](https://doi.org/10.1086/430347)
- J. Andries, I. Arregui, M. Goossens, Astron. Astrophys. **497**, 265–272 (2009). doi:[10.1051/0004-6361/200811481](https://doi.org/10.1051/0004-6361/200811481)
- J. Andries, M. Goossens, J. Hollweg, I. Arregui, T. Van Doorsselaere, Astron. Astrophys. **430**, 1109–1118 (2005). doi:[10.1051/0004-6361:20041832](https://doi.org/10.1051/0004-6361:20041832)
- I. Arregui, T. Van Doorsselaere, J. Andries, M. Goossens, D. Kimpe, Astron. Astrophys. **441**, 361–370 (2005). doi:[10.1051/0004-6361:20053039](https://doi.org/10.1051/0004-6361:20053039)
- I. Arregui, T. Van Doorsselaere, J. Andries, M. Goossens, Philos. Trans. R. Soc. A **364**, 529–532 (2006). doi:[10.1098/rsta.2005.1714](https://doi.org/10.1098/rsta.2005.1714)

- M.J. Aschwanden, J. Terradas, *Astrophys. J.* **686**(2), L127–L130 (2008). doi:[10.1086/592963](https://doi.org/10.1086/592963)
- M.J. Aschwanden, L. Fletcher, C.J. Schrijver, D. Alexander, *Astrophys. J.* **520**(2), 880–894 (1999). doi:[10.1086/307502](https://doi.org/10.1086/307502)
- M.J. Aschwanden, B. de Pontieu, C.J. Schrijver, A.M. Title, *Solar Phys.* **206**(1), 99–132 (2002). doi:[10.1023/A:1014916701283](https://doi.org/10.1023/A:1014916701283)
- M.J. Aschwanden, L.F. Burlaga, M.L. Kaiser, C.K. Ng, D.V. Reames, M.J. Reiner, T.I. Gombosi, N. Lugaz, W. Manchester, I.I. Roussev, T.H. Zurbuchen, C.J. Farrugia, A.B. Galvin, M.A. Lee, J.A. Linker, Z. Mikić, P. Riley, D. Alexander, A.W. Sandman, J.W. Cook, R.A. Howard, D. Održić, V.J. Pizzo, J. Kóta, P.C. Liewer, J.G. Luhmann, B. Inhester, R.W. Schwenn, S.K. Solanki, V.M. Vasiliu, T. Wiegelmann, L. Blush, P. Bochsler, I.H. Cairns, P.A. Robinson, V. Bothmer, K. Kecskemeti, A. Llebaria, M. Maksimovic, M. Scholer, R.F. Wimmer-Schweingruber, *Space Sci. Rev.* **136**(1–4), 565–604 (2008). doi:[10.1007/s11214-006-9027-8](https://doi.org/10.1007/s11214-006-9027-8)
- M. Aschwanden, R. Nightingale, J. Andries, M. Goossens, T. Van Doorsselaere, *Astrophys. J.* **598**, 1375–1386 (2003). doi:[10.1086/379104](https://doi.org/10.1086/379104)
- P.S. Cally, *Solar Phys.* **103**(2), 277–298 (1986). doi:[10.1007/BF00147830](https://doi.org/10.1007/BF00147830)
- F.C. Cooper, V.M. Nakariakov, D. Tsiklauri, *Astron. Astrophys.* **397**(2), 765–770 (2003). doi:[10.1051/0004-6361:20021556](https://doi.org/10.1051/0004-6361:20021556)
- I. De Moortel, C.S. Brady, *Astrophys. J.* **664**(2), 1210–1213 (2007). doi:[10.1086/518830](https://doi.org/10.1086/518830)
- C.E. DeForest, *Astrophys. J.* **661**(1), 532–542 (2007). doi:[10.1086/515561](https://doi.org/10.1086/515561)
- A.J. Díaz, G.R. Donnelly, B. Roberts, *Astron. Astrophys.* **476**(1), 359–368 (2007). doi:[10.1051/0004-6361:20078385](https://doi.org/10.1051/0004-6361:20078385)
- A.J. Díaz, R. Oliver, J.L. Ballester, *Astrophys. J.* **580**(1), 550–565 (2002). doi:[10.1086/343039](https://doi.org/10.1086/343039)
- A.J. Díaz, R. Oliver, J.L. Ballester, *Astrophys. J.* **645**(1), 766–775 (2006). doi:[10.1086/504145](https://doi.org/10.1086/504145)
- A.J. Díaz, R. Oliver, J.L. Ballester, B. Roberts, *Astron. Astrophys.* **424**(3), 1055–1064 (2004). doi:[10.1051/0004-6361:20035707](https://doi.org/10.1051/0004-6361:20035707)
- G.R. Donnelly, A.J. Díaz, B. Roberts, *Astron. Astrophys.* **457**(2), 707–715 (2006). doi:[10.1051/0004-6361:20065524](https://doi.org/10.1051/0004-6361:20065524)
- G.R. Donnelly, A.J. Díaz, B. Roberts, *Astron. Astrophys.* **471**(3), 999–1009 (2007). doi:[10.1051/0004-6361:20066094](https://doi.org/10.1051/0004-6361:20066094)
- M.V. Dymova, M.S. Ruderman, *Solar Phys.* **229**(1), 79–94 (2005). doi:[10.1007/s11207-005-5002-x](https://doi.org/10.1007/s11207-005-5002-x)
- M.V. Dymova, M.S. Ruderman, *Astron. Astrophys.* **459**(1), 241–244 (2006). doi:[10.1051/0004-6361:20065929](https://doi.org/10.1051/0004-6361:20065929)
- M.V. Dymova, M.S. Ruderman, *Astron. Astrophys.* **457**(3), 1059–1070 (2006). doi:[10.1051/0004-6361:20065051](https://doi.org/10.1051/0004-6361:20065051)
- P.M. Edwin, B. Roberts, *Solar Phys.* **88**, 179–191 (1983). doi:[10.1007/BF00196186](https://doi.org/10.1007/BF00196186)
- R. Erdélyi, R.J. Morton, *Astron. Astrophys.* **494**(2), 295–309 (2009). doi:[10.1051/0004-6361:200810318](https://doi.org/10.1051/0004-6361:200810318)
- R. Erdélyi, G. Verth, *Astron. Astrophys.* **462**(2), 743–751 (2007). doi:[10.1051/0004-6361:20065693](https://doi.org/10.1051/0004-6361:20065693)
- G.A. Gary, *Solar Phys.* **174**(1/2), 241–263 (1997). doi:[10.1023/A:1004978630098](https://doi.org/10.1023/A:1004978630098)
- J.P. Goedbloed, S. Poedts, *Principles of magnetohydrodynamics* (Cambridge University Press, Cambridge, 2004). ISBN 0521626072
- M. Goossens, J. Andries, I. Arregui, *Philos. Trans. R. Soc. A* **364**, 433–445 (2006). doi:[10.1098/rsta.2005.1708](https://doi.org/10.1098/rsta.2005.1708)
- M. Goossens, J. Andries, M. Aschwanden, *Astron. Astrophys.* **394**, L39–L42 (2002). doi:[10.1051/0004-6361:20021378](https://doi.org/10.1051/0004-6361:20021378)
- D.B. Jess, M. Mathioudakis, R. Erdélyi, G. Verth, R.T.J. McAteer, F.P. Keenan, *Astrophys. J.* **680**(2), 1523–1531 (2008). doi:[10.1086/587735](https://doi.org/10.1086/587735)
- J.A. Klimchuk, S.K. Antiochos, D. Norton, *Astrophys. J.* **542**(1), 504–512 (2000). doi:[10.1086/309527](https://doi.org/10.1086/309527)
- J. Klimchuk, *Solar Phys.* **193**(1/2), 53–75 (2000). doi:[10.1023/A:1005210127703](https://doi.org/10.1023/A:1005210127703)
- J. Lighthill, *Waves in fluids* (Cambridge University Press, Cambridge, 1978)
- H. Lin, J.R. Kuhn, R. Coulter, *Astrophys. J.* **613**(2), L177–L180 (2004). doi:[10.1086/425217](https://doi.org/10.1086/425217)
- M.C. López Fuentes, P. Démoulin, J.A. Klimchuk, *Astrophys. J.* **673**(1), 586–597 (2008). doi:[10.1086/523928](https://doi.org/10.1086/523928)
- M.C. López Fuentes, J.A. Klimchuk, P. Démoulin, *Astrophys. J.* **639**(1), 459–474 (2006). doi:[10.1086/499155](https://doi.org/10.1086/499155)
- A.N. McClymont, Z. Mikic, *Astrophys. J.* **422**, 899–905 (1994). doi:[10.1086/173781](https://doi.org/10.1086/173781)
- M.P. McEwan, A.J. Díaz, *Solar Phys.* **246**, 243–257 (2007). doi:[10.1007/s11207-007-0395-3](https://doi.org/10.1007/s11207-007-0395-3)
- M.P. McEwan, A.J. Díaz, B. Roberts, *Astron. Astrophys.* **481**(3), 819–825 (2008). doi:[10.1051/0004-6361:20078016](https://doi.org/10.1051/0004-6361:20078016)
- M.P. McEwan, G.R. Donnelly, A.J. Díaz, B. Roberts, *Astron. Astrophys.* **460**(3), 893–899 (2006). doi:[10.1051/0004-6361:20065313](https://doi.org/10.1051/0004-6361:20065313)

- V.F. Melnikov, V.E. Reznikova, K. Shibasaki, V.M. Nakariakov, *Astron. Astrophys.* **439**, 727–736 (2005). doi:[10.1051/0004-6361:20052774](https://doi.org/10.1051/0004-6361:20052774)
- R.J. Morton, R. Erdélyi, *Astron. Astrophys.* (2009). doi:[10.1051/0004-6361/200811405](https://doi.org/10.1051/0004-6361/200811405)
- V.M. Nakariakov, L. Ofman, *Astron. Astrophys.* **372**(3), L53–L56 (2001). doi:[10.1051/0004-6361:20010607](https://doi.org/10.1051/0004-6361:20010607)
- V.M. Nakariakov, V.F. Melnikov, V.E. Reznikova, *Astron. Astrophys.* **412**(1), L7–L10 (2003). doi:[10.1051/0004-6361:20031660](https://doi.org/10.1051/0004-6361:20031660)
- V.M. Nakariakov, L. Ofman, E.E. Deluca, B. Roberts, J.M. Davila, *Science* **285**(5429), 862–864 (1999). doi:[10.1126/science.285.5429.862](https://doi.org/10.1126/science.285.5429.862)
- E. O’Shea, A.K. Srivastava, J.G. Doyle, D. Banerjee, *Astron. Astrophys.* **473**(2), 13–16 (2007). doi:[10.1051/0004-6361:20078122](https://doi.org/10.1051/0004-6361:20078122)
- B. Roberts, A.R. Webb, *Solar Phys.* **56**(1), 5–35 (1978). doi:[10.1007/BF00152630](https://doi.org/10.1007/BF00152630)
- B. Roberts, A.R. Webb, *Solar Phys.* **64**(1), 77–92 (1979). doi:[10.1007/BF00151117](https://doi.org/10.1007/BF00151117)
- B. Roberts, P.M. Edwin, A.O. Benz, *Astrophys. J.* **279**, 857–865 (1984). doi:[10.1086/161956](https://doi.org/10.1086/161956)
- M.S. Ruderman, *Astron. Astrophys.* **409**(1), 287–297 (2003). doi:[10.1051/0004-6361:20031079](https://doi.org/10.1051/0004-6361:20031079)
- M.S. Ruderman, R. Erdélyi, *Space Sci. Rev.* (2009). doi:[10.1007/s11214-009-9535-u](https://doi.org/10.1007/s11214-009-9535-u)
- M.S. Ruderman, B. Roberts, *Astrophys. J.* **577**(1), 475–486 (2002). doi:[10.1086/342130](https://doi.org/10.1086/342130)
- M.S. Ruderman, G. Verth, R. Erdélyi, *Astrophys. J.* **686**(1), 694–700 (2008). doi:[10.1086/591444](https://doi.org/10.1086/591444)
- D.D. Ryutov, M.P. Ryutova, *Sov. Phys. JETP* **43**, 491 (1976)
- H. Safari, S. Nasiri, Y. Sobouti, *Astron. Astrophys.* **470**(3), 1111–1116 (2007). doi:[10.1051/0004-6361:20065997](https://doi.org/10.1051/0004-6361:20065997)
- J.D. Scargle, *Astrophys. J. Suppl. Ser.* **45**, 1–71 (1981). doi:[10.1086/190706](https://doi.org/10.1086/190706)
- C.J. Schrijver, A.M. Title, T.E. Berger, L. Fletcher, N.E. Hurlburt, R.W. Nightingale, R.A. Shine, T.D. Tarbell, J. Wolfson, L. Golub, J.A. Bookbinder, E.E. Deluca, R.A. McMullen, H.P. Warren, C.C. Kankelborg, B.N. Handy, B. de Pontieu, *Solar Phys.* **187**(2), 261–302 (1999). doi:[10.1023/A:1005194519642](https://doi.org/10.1023/A:1005194519642)
- C.J. Schrijver, M.J. Aschwanden, A.M. Title, *Solar Phys.* **206**(1), 69–98 (2002). doi:[10.1023/A:1014957715396](https://doi.org/10.1023/A:1014957715396)
- M. Selwa, S.K. Solanki, K. Murawski, T.J. Wang, U. Shumlak, *Astron. Astrophys.* **454**(2), 653–661 (2006). doi:[10.1051/0004-6361:20054286](https://doi.org/10.1051/0004-6361:20054286)
- H.C. Spruit, *Solar Phys.* **75**, 3–17 (1982). doi:[10.1007/BF00153456](https://doi.org/10.1007/BF00153456)
- A.K. Srivastava, T.V. Zaqarashvili, W. Uddin, B.N. Dwivedi, P. Kumar, *Mon. Not. R. Astron. Soc. Lett.* **388**(4), 1899–1903 (2008). doi:[10.1111/j.1365-2966.2008.13532.x](https://doi.org/10.1111/j.1365-2966.2008.13532.x)
- J. Terradas, J. Andries, M. Goossens, *Astron. Astrophys.* **469**, 1135–1143 (2007). doi:[10.1051/0004-6361:20077404](https://doi.org/10.1051/0004-6361:20077404)
- J. Terradas, R. Oliver, J.L. Ballester, *Astrophys. J.* **614**(1), 435–447 (2004). doi:[10.1086/423332](https://doi.org/10.1086/423332)
- J. Terradas, R. Oliver, J.L. Ballester, *Astrophys. J.* **650**, L91–L94 (2006). doi:[10.1086/508569](https://doi.org/10.1086/508569)
- C. Torrence, G.P. Compo, *Bull. Am. Meteorol. Soc.* **79**, 61–78 (1998). doi:[10.1175/1520-0477\(1998\)079<0061:CTGPAE>2.0.CO;2](https://doi.org/10.1175/1520-0477(1998)079<0061:CTGPAE>2.0.CO;2)
- T. Van Doorsselaere, J. Andries, S. Poedts, *Astron. Astrophys.* **471**, 311–314 (2007). doi:[10.1051/0004-6361:20066658](https://doi.org/10.1051/0004-6361:20066658)
- T. Van Doorsselaere, V. Nakariakov, E. Verwichte, *Astron. Astrophys.* **473**(3), 959–966 (2007). doi:[10.1051/0004-6361:20077783](https://doi.org/10.1051/0004-6361:20077783)
- T. Van Doorsselaere, A. Debosscher, J. Andries, S. Poedts, *Astron. Astrophys.* **424**, 1065–1074 (2004). doi:[10.1051/0004-6361:20041239](https://doi.org/10.1051/0004-6361:20041239)
- T. Van Doorsselaere, E. Verwichte, J. Terradas, *Space Sci. Rev.* (2009). doi:[10.1007/s11214-009-9530-9](https://doi.org/10.1007/s11214-009-9530-9)
- G. Verth, R. Erdélyi, *Astron. Astrophys.* **486**(3), 1015–1022 (2008). doi:[10.1051/0004-6361:200809626](https://doi.org/10.1051/0004-6361:200809626)
- G. Verth, R. Erdélyi, D.B. Jess, *Astrophys. J.* **687**(1), L45–L48 (2008). doi:[10.1086/593184](https://doi.org/10.1086/593184). <http://www.journals.uchicago.edu/doi/abs/10.1086/593184>
- G. Verth, T. Van Doorsselaere, R. Erdélyi, M. Goossens, *Astron. Astrophys.* **475**(1), 341–348 (2007). doi:[10.1051/0004-6361:20078086](https://doi.org/10.1051/0004-6361:20078086)
- E. Verwichte, V.M. Nakariakov, L. Ofman, E.E. Deluca, *Solar Phys.* **223**, 77–94 (2004). doi:[10.1007/s11207-004-0807-6](https://doi.org/10.1007/s11207-004-0807-6)
- E. Verwichte, M.J. Aschwanden, T. Van Doorsselaere, C. Foullon, V.M. Nakariakov, *Astrophys. J.* **698**, 397–404 (2009). doi:[10.1088/0004-637X/698/1/397](https://doi.org/10.1088/0004-637X/698/1/397)
- T.J. Wang, S.K. Solanki, M. Selwa, *Astron. Astrophys.* **489**(3), 1307–1317 (2008). doi:[10.1051/0004-6361:200810230](https://doi.org/10.1051/0004-6361:200810230)
- J. Watko, J.A. Klimchuk, *Solar Phys.* **193**(1/2), 77–92 (2000). doi:[10.1023/A:1005209528612](https://doi.org/10.1023/A:1005209528612)
- D.G. Wentzel, *Astron. Astrophys.* **76**, 20–23 (1979)
- P.R. Wilson, *Astron. Astrophys.* **71**, 9–13 (1979)
- P.R. Wilson, *Astron. Astrophys.* **87**, 121–125 (1980)
- V.V. Zaitsev, A.V. Stepanov, *Issled. Geomagn. Aeron. Fiz. Solntsa* **3** (1975)